isolated using a Quantum Prep Plasmid Maxiprep kit (Bio-Rad Laboratories, Hercules, CA, USA). Next, human IL8 cDNAs were amplified from Cos-7 cells cDNA using the primers: (5′-gaGAA TTCATTTAAATgacttccaagctggccgtggct-3′ and 5′-gcagcatcGCGGCCGCtgaattctcagccctcttc aaaaa-3′), as described above. These were inserted into the pCAGGS-glucagon 19-29 vector using the SwaI and NotI sites and the recombinant plasmids, i.e., pCAGGS-IL8 glucagon 19-29, were isolated as described above.

To construct a negative control plasmid, i.e., pCAGGS-IFN gamma receptor extracellular domain (ECD) IgG-Fc without glucagon 19-29, rat IgG1Fc cDNAs were amplified from rat spleen cDNA using the primers: (5′-gaGAATTCATT TAAATgagaGCGGCCGCcgtgcccagaaactgtg-3′ with SwaI and NotI restriction sites and 5′-gagagagaGAATTCactctggggtcatttacccggagag tgggag-3′) (Bruggemann et al. 1986) as described above. The amplified cDNA was inserted into the pCAGGS vector using the EcoRI sites. Escherichia coli JM109 competent cells were then transformed and recombinant plasmids, i.e., pCAGGS-rat IgG-Fc were isolated as described above. Next, rat IFN gamma receptor ECD cDNAs were amplified using the primers: (5′-gaGAATTCATT TAAATgattctgctggtggtcctgatg-3′ and 5′-gcagcatcGCGGCCGCttcttctctgtcatcatggagaaa-3′), as described above. These products were inserted into the pCAGGS-rat IgG-Fc vector using the SwaI and NotI sites and the recombinant plasmids, i.e., pCAGGS-IFN gamma receptor ECD IgG-Fc without glucagon 19-29, were isolated as described above.

To construct the plasmid pCAGGS-IFN gamma receptor ECD IgG-Fc glucagon 19-29, the first PCR products were amplified from the diluted negative control plasmid using the primers: (5′-gaGAATTCATTTAAATgagaGCGGCCGCc gtgcccagaaactgtg-3′, 5′-tcaaccactgcacaaaatcttgg gcTTTACCCGGAGAGTGGGAGAGACT-3′) as described above. The final PCR product inserts were then amplified from the diluted products of the first PCR reaction with the primers: (5′-gaGAATTCATTTAAATgagaGCGGCCGCcgtgc ccagaaactgtg-3′ and 5′-gagagagaGAATTCtcaggta ttcatcaaccactgcacaaaatcttgggc-3′) (Heinrich et al. 1984). These products were inserted into the pCAGGS vector using EcoRI sites. The recombinant plasmids, i.e., pCAGGS-IFN gamma receptor ECD IgG-Fc glucagon 19-29, were then isolated as described above.

Rats

Eight-week-old male Lewis rats were purchased from Charles-River Japan, Inc. (Tokyo). One week later, we injected plasmid DNA into nine-week-old rats. Throughout the studies, all the animals were treated in accordance with the guidelines for animal experiments of our institute.

Gene transfer and assay of synthesized protein in blood

To compare IL8 glucagon 19-29 concentrations in blood calculated using glucagon tag and using IL8, eight rats were injected with 400 μg of pCAGGS-IL8 glucagon 19-29 which were added to 20 ml volumes of Ringer solution via the tail vein within 15 seconds (receiving approximately 80 ml/kg body weight) (Maruyama et al. 2002). Blood samples were taken 24 hours following injection. Glucagon concentrations were measured using a glucagon RIA Kit (DAIICHI RADIOISOTOPE LABS, Tokyo) (Imagawa et al. 1979; Nishino et al. 1981) and IL8 concentrations using IL-8 EASIA (BIOSOURCE, Nivelles, Belgium).

To measure rat IFN gamma receptor ECD IgG-Fc glucagon protein and blood sugar concentrations throughout the acute phase, ten rats were divided into two groups, a Glucagon 19-29 positive group (treated with plasmid pCAGGS-IFN gamma receptor ECD IgG-Fc glucagon 19-29, n=5), and a Glucagon 19-29 negative group (treated with plasmid pCAGGS-IFN gamma receptor ECD IgG-Fc, n=5). The plasmids (800 μg each) were added to 20 ml volume of Ringer solution and rats were injected via the tail vein within

15 seconds (receiving approximately 80 ml/kg body weight) (Maruyama et al. 2002). Blood samples were taken 4 hours, 8 hours, and 12 hours following injection. Glucagon concentrations were measured from 10 μl plasma samples diluted with 50-100 PBS using a glucagon RIA Kit as described above. Blood sugar was measured using a glutestsensor (SANWA KAGAKU KENKYUSHO, Nagoya).

To measure synthesized protein concentrations at subsequent time points, seven rats were injected with the plasmid pCAGGS-IFN gamma receptor ECD IgG-Fc glucagon 19-29 and three rats were injected with the control plasmid pCAGGS-IFN gamma receptor ECD IgG-Fc as described above. Blood samples were taken 1, 3, 7 and 16 days after injection, and glucagon concentrations were measured as described above.

Results

Synthesized protein concentration in blood and blood sugar levels

Human IL8 glucagon 19-29 protein concentrations 24 hours after injection of pCAGGS-IL8 glucagon 19-29 calculated using glucagon were similar to those using human IL8 (Fig. 1).

During the acute phase, IFN gamma receptor ECD IgG-Fc glucagon 19-29 concentrations were 2815±2318 ng/ml (mean±S.D.) 4 hours after injection of pCAGGS-IFN gamma receptor ECD IgG-Fc glucagon 19-29, 6061±2789 ng/ml 8 hours after injection, and 5752±2270 ng/ml 12 hours after injection. The protein concentration peaked at 8 hours and the protein concentrations in the Glucagon 19-29 negative group were not detected at any point (Fig. 2). The differences between blood sugar in the Glucagon 19-29 negative group and the Glucagon 19-29 positive group after 4

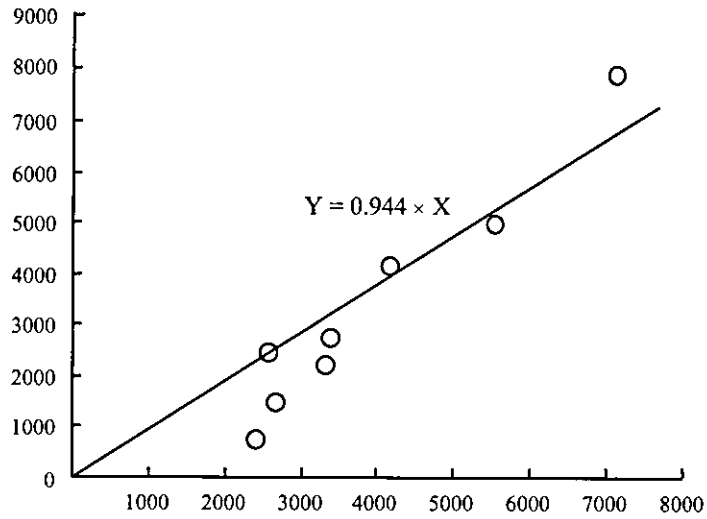

Fig. 1. The chimeric protein (human IL8 glucagon 19-29) concentrations calculated using glucagon or human IL8 in blood 24 hours after injection of plasmids.
Chimera protein (human IL8 glucagon 19-29) concentrations were calculated using the following formula: (human IL8 glucagon 19-29 protein concentration)=(actually measured glucagon concentration)×(human IL8 glucagon 19-29 protein molecular weight)/(whole glucagon molecular weight), or (human IL8 glucagon 19-29 protein concentration)=(actually measured human IL-8 concentration)×(human IL8 glucagon 19-29 protein molecular weight)/(whole human IL-8 molecular weight) Regression line: Y=0.944×X.

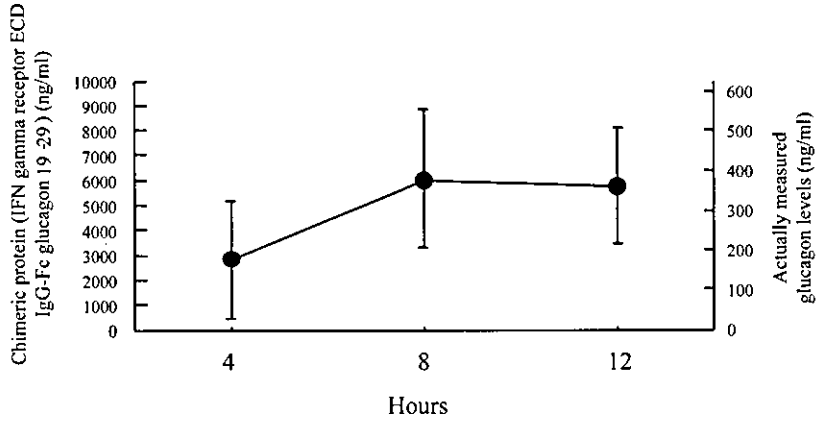

Fig. 2. The chimeric protein (IFN gamma receptor ECD IgG-Fc glucagon 19-29) concentrations in blood during the acute phase following injection of plasmids. Chimeric proteins were not indicated by increased glucagon antigen levels in the blood of any rat in the control (Glucagon 19-29 negative) group (data not shown). Chimera protein (IFN gamma receptor ECD IgG-Fc glucagon 19-29) concentrations were calculated using the following formula: (IFN gamma receptor ECD IgG-Fc glucagon 19-29 protein concentration)=(actually measured glucagon concentration) ×(IFN gamma receptor ECD IgG-Fc glucagon 19-29 protein molecular weight)/(whole glucagon molecular weight).

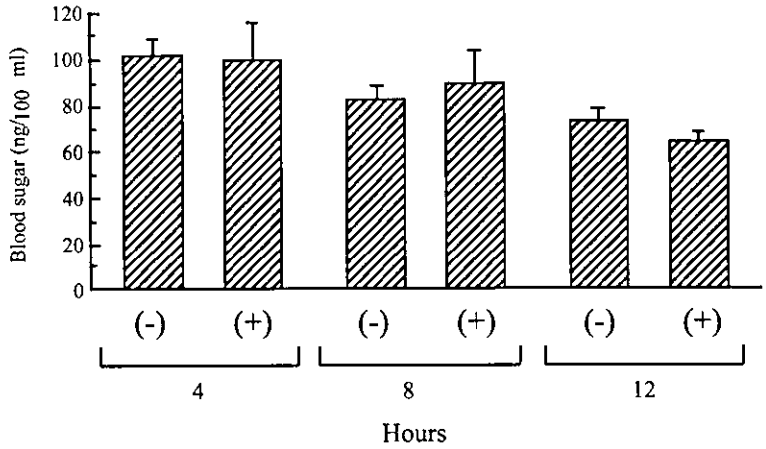

Fig. 3. Blood sugar levels following gene therapy. Differences between the Glucagon 19-29 positive group and the Glucagon 19-29 negative group were not significant at any time. The symbol "(+)" denotes the Glucagon 19-29 positive group and the symbol "(−)" denotes the Glucagon 19-29 negative group.

hours (100.6±8.8 mg/100 ml vs 99.0±17.5 mg/100 ml), 8 hours (81.8±7.5 mg/100 ml vs 89.3±15.1 mg/100 ml), and 12 hours (71.4±6.9 mg/100 ml vs 63.5±5.7 mg/100 ml) were not significant (Fig. 3).

At later time points, the synthesized protein concentrations decreased gradually: 2870±1062 ng/ml after one day, 1440±334 ng/ml after three days, 1120±433 ng/ml after seven days, and 281± 162 ng/ml after 16 days. Chimeric protein levels in diluted plasma samples from rats treated with the control plasmid (without glucagon residues 19-29) were below the detection levels of this assay (Fig. 4).

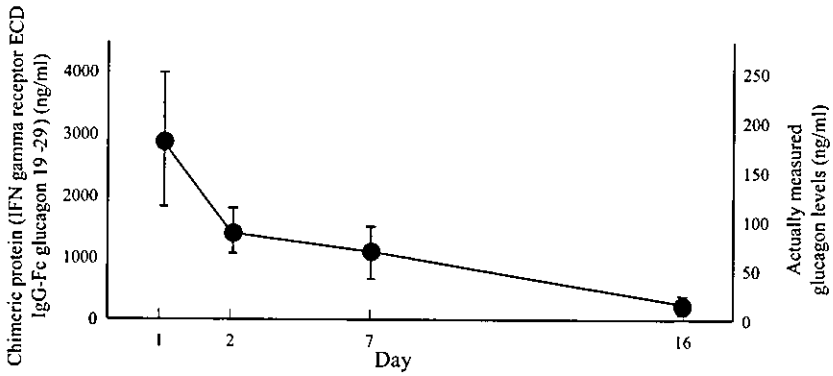

Fig. 4. Chimeric protein (IFN gamma receptor ECD IgG-Fc glucagon 19-29) levels in plasma of the Glucagon 19-29 positive group decreased following the acute phase. Chimeric proteins were not indicated by increased glucagon antigen levels in the blood of any rat in the control (Glucagon 19-29 negative) group (data not shown).

Discussion

The chimeric recombinant protein with a C-terminal tag consisting of glucagon residues 19-29 synthesized as a result of this gene therapy protocol could be measured using an RIA-based method for 16 days following injection of plasmid vectors into rats. This tag was detected by RIA, which also reacted with endogenous glucagon. The normal range of glucagon concentration in humans is 0.023-0.197 ng/ml. Glucagon antigen was detected at levels far above endogenous glucagon levels for 16 days following injection of the protein expression plasmid. Glucagon levels in blood were too low to be detected in any of the 50-100 diluted plasma samples taken from rats that received a control plasmid encoding the protein minus the glucagon tag. Therefore, we concluded that the glucagon levels measured for the Glucagon 19-29 positive rats accurately reflected the concentrations of the synthesized recombinant protein. Peak chimera protein synthesis in the Glucagon 19-29 positive group occurred eight hours following plasmid injection. Therefore, protein synthesis after intravenous injection of plasmid DNA into rats may begin earlier than in vitro transfection. Blood sugar levels in this group did not rise, even during the acute phase, indicating that the recombinant tag did not cause the type of physiological response that would be expected following a rise in normal glucagon levels. This implies that the Glucagon 19-29 tag will be useful and well tolerated in other gene therapy protocols. Injection of naked plasmid into the muscle or vein is an easy and cheap gene therapy method that is being explored in many laboratories. The synthesized protein levels following these protocols, however, can vary significantly between different animals. In gene therapy, the accurate measurement of synthesized protein in blood is essential to investigate the effects and side effects of the therapy. We present here a novel and convenient method to assay expression of gene therapy protein products, through use of a glucagon residue 19-29 C-terminal protein tag.

References

Bouchard, B.A., Furie, B. & Furie, B.C. (1999) Glutamyl substrate-induced exposure of a free cysteine residue in the vitamin K-dependent gamma-glutamyl carboxylase is critical for vitamin K epoxidation. *Biochemistry*, **38**, 9517-9523.

Bruggemann, M., Free, J., Diamond, A., Howard, J., Cobbold, S. & Waldmann, H. (1986) Immunoglobulin heavy chain locus of the rat: striking homology to mouse antibody genes. *Proc. Natl. Acad. Sci. USA*, **83**, 6075-6079.

Denbow, C.J., Lang, S. & Cramer, C.L. (1996) The N-terminal domain of tomato 3-hydroxy-3-

methylglutaryl-CoA reductases. Sequence, microsomal targeting, and glycosylation. *J. Biol. Chem.*, **271**, 9710-9715.

Hefti, M.H., Milder, F.J., Boeren, S., Vervoort, J. & van Berkel, W.J. (2003) A His-tag based immobilization method for the preparation and reconstitution of apoflavoproteins. *Biochim. Biophys. Acta*, **1619**, 139-143.

Heinrich, G., Gros, P. & Habener, J.F. (1984) Glucagon gene sequence. Four of six exons encode separate functional domains of rat pre-proglucagon. *J. Biol. Chem.*, **259**, 14082-14087.

Imagawa, K., Nishino, T., Shin, S., Uehata, S., Hashimura, E., Yanaihara, C. & Yanaihara, N. (1979) Production of anti-glucagon sera with a C-terminal fragment of pancreatic glucagon. *Endocrinol. Jpn.*, **26**, 123-131.

Irwin, D.M. (2001) Molecular evolution of proglucagon. *Regul. Pept.*, **98**, 1-12.

Lawson, B.R., Prud'homme, G.J., Chang, Y., Gardner, H.A., Kuan, J., Kono, D.H. & Theofilopoulos, A.N. (2000) Treatment of murine lupus with cDNA encoding IFN-gammaR/Fc. *J. Clin. Invest.*, **106**, 207-215.

Lefebvre, P.J. (1995) Glucagon and its family revisited. *Diabetes Care*, **18**, 715-730.

Liu, F., Song, Y. & Liu, D. (1999) Hydrodynamics-based transfection in animals by systemic administration of plasmid DNA. *Gene Ther.*, **6**, 1258-1266.

Lu, Q., Bauer, J.C. & Greener, A. (1997) Using Schizosaccharomyces pombe as a host for expression and purification of eukaryotic proteins. *Gene*, **200**, 135-144.

Maruyama, H., Higuchi, N., Nishikawa, Y., Kameda, S., Iino, N., Kazama, J.J., Takahashi, N., Sugawa, M., Hanawa, H., Tada, N., Miyazaki, J. & Gejyo, F. (2002) High-level expression of naked DNA delivered to rat liver via tail vein injection. *J. Gene. Med.*, **4**, 333-341.

Matsui, Y., Inobe, M., Okamoto, H., Chiba, S., Shimizu, T., Kitabatake, A. & Uede, T. (2002) Blockade of T cell Costimulatory Signals using Adenovirus Vectors Prevents both the Induction and the Progression of Experimental Autoimmune Myocarditis. *J. Mol. Cell. Cardiol.*, **34**, 279-295.

Nishino, T., Kodaira, T., Shin, S., Imagawa, K., Shima, K., Kumahara, Y., Yanaihara, C. & Yanaihara, N. (1981) Glucagon radioimmunoassay with use of antiserum to glucagon C-terminal fragment. *Clin. Chem.*, **27**, 1690-1697.

Quattrocchi, E., Dallman, M.J. & Feldmann, M. (2000) Adenovirus-mediated gene transfer of CTLA-4Ig fusion protein in the suppression of experimental autoimmune arthritis. *Arthritis. Rheum.*, **43**, 1688-1697.

Watanabe, K., Nakazawa, M., Fuse, K., Hanawa, H., Kodama, M., Aizawa, Y., Ohnuki, T., Gejyo, F., Maruyama, H. & Miyazaki, J. (2001) Protection against autoimmune myocarditis by gene transfer of interleukin-10 by electroporation. *Circulation*, **104**, 1098-1100.

Virchows Arch (2004) 444:283–292
DOI 10.1007/s00428-003-0925-9

ORIGINAL ARTICLE

Takeshi Kashimura · Makoto Kodama · Yuko Hotta · Junichi Hosoya · Kaori Yoshida · Takuya Ozawa · Ritsuo Watanabe · Yuji Okura · Kiminori Kato · Haruo Hanawa · Ryozo Kuwano · Yoshifusa Aizawa

Spatiotemporal changes of coxsackievirus and adenovirus receptor in rat hearts during postnatal development and in cultured cardiomyocytes of neonatal rat

Received: 9 July 2003 / Accepted: 7 October 2003 / Published online: 18 November 2003

Abstract Coxsackievirus B is the most common cause of viral myocarditis and is particularly virulent in neonates and children. Adenovirus is also a leading cause of the disease. The determinant of tropism for both viruses is considered to be the expression of coxsackievirus and adenovirus receptor (CAR) in target organs. However, developmental change and physiological localization of CAR in the heart are unknown. We examined expression levels of CAR in rat hearts by quantitative real-time polymerase chain reaction and Western blot analysis and found that CAR decreased gradually during postnatal development, although CAR was detectable, even in adults. Immunohistochemistry revealed CAR on the whole surface of cardiomyocytes in immature rat hearts. In contrast, CAR was detected predominantly on intercalated disks in the adult heart and was accumulated especially at the contact point between the cultured cardiomyocytes, even though they were prepared from the neonatal rat heart. In conclusion, CAR was expressed abundantly on the whole surface of cardiomyocytes in immature rat hearts. Both the expression level and the localization of CAR are possible determinants of the susceptibility to viral myocarditis of neonates and children.

T. Kashimura (✉) · M. Kodama · K. Yoshida · T. Ozawa · R. Watanabe · Y. Okura · K. Kato · H. Hanawa · Y. Aizawa
Division of Cardiology,
Niigata University Graduate School of Medical and Dental Sciences,
1-754 Asahimachi, 951-8510 Niigata, Japan
e-mail: kashi@med.niigata-u.ac.jp
Tel.: +81-25-2272185
Fax: +81-25-2270774

Y. Hotta · J. Hosoya · R. Kuwano
Genome Science Branch,
Center for Bioresource-Based Researches,
Brain Research Institute, Niigata University,
Niigata, Japan

Keywords Coxsackievirus and adenovirus receptor · Myocarditis · Development · Cardiomyocyte · Intercalated disk

Introduction

Acute myocarditis leads to heart failure and sudden death. The chronic type leads to dilated cardiomyopathy, and both remain major causes of morbidity and mortality, particularly in neonates and children [3, 7, 18, 26, 29]. However, the susceptibility to viral myocarditis at early ages has not been elucidated.

Coxsackievirus B [17, 21] and adenovirus [16] are leading causes of viral myocarditis in humans. It is also well known that acute myocarditis can be produced in neonatal and young mice experimentally with coxsackievirus B [12]. The first step of viral infection requires the binding of virus particles to specific cell surface receptors [37]. Interestingly, the two viruses share a common receptor: the coxsackievirus and adenovirus receptor (CAR) [2, 4, 32].

We reported that CAR plays a role in homophilic cell–cell contact[13] and is expressed in the newborn brain and the heart of rodents [13, 14], but the physiological function of CAR has not yet been clarified. However, CAR has been shown to be an important determinant of efficiency of gene transfer using adenovirus vectors: the expression of CAR in target cells or organs enhanced adenoviral gene transfer in both in vitro and in vivo studies [8, 15, 19, 20, 36]. However, the localization, not the expression level, of CAR is considered much more important for infection [6, 9, 25, 33, 34, 35].

Therefore, CAR is currently related to coxsackievirus and adenovirus myocarditis and adenovirus-mediated gene therapy [27]. While cardiac CAR was formerly reported to be unchanged from neonate to adult [19], recent studies suggested a decrease in adult CAR [10, 14], and the localization of CAR in the heart needs to be

Table 1 Primers used for polymerase chain reaction (PCR) and quantitative real-time PCR (qPCR). *CAR* coxsackievirus and adenovirus receptor

	Primer sequence	Number	Product
CAR1 (PCR)	gaacagaggatcgaaaaagctaaag cattcgacttagattaggggcag	AF109644	969 bp
CAR2 (PCR)	gaacagaggatcgaaaaagctaaag ggtaagcgtacttgaact	AF109643	957 bp
CAR1 (qPCR)	catcctcttctgctgtcataaaaa cattcgacttagattaggggcag	AF109644	280 bp
CAR2 (qPCR)	ctgtcatagggacgctgctt gtaagcgtacttgaact	AF109643	306 bp
ANP	atggatttcaagaacctgctagac gctccaatcctgtcaatcctac	E00698	308 bp
α-Cardiac myosin	acaaggttaaaaacctgacagagg tactgttctgctgactgatgtcaa	X15938	360 bp
N-cadherin	gtcaatgaaaatccttattttgcc aagtaaatagatttgcagcgttcc	X06656	318 bp
Connexin43	aagttcaagtacgggattgaagag gcctttgaagaagacgtagaagag	AB017695	306 bp

studied. We reported that neonatal rat hearts exhibited higher immunoreactivity to anti-CAR antibodies than those of adult hearts [14], but did not focus on the precise localization. CAR was re-expressed on the cell surface of myocytes in diseased hearts, such as explanted human hearts from patients with dilated cardiomyopathy [22] and a rat model of myocardial infarction [10]. However, physiological localization and its developmental change have not been examined. In the present study, we reconfirmed the developmental changes of CAR expression, not only mRNA expression, but also protein expression, in rat hearts, and then, spatiotemporal change of CAR was studied in vivo and in vitro. To avoid nonspecific staining of CAR, we used three anti-CAR antibodies.

Materials and methods

Experimental animals

Lewis rats in the late stage of pregnancy were purchased from Charles River, Japan (Yokohama, Kanagawa, Japan). Newborn rats were fed by their own parents and maintained in our animal facilities. The "Principals of laboratory animal care" (NIH publication no. 85–23, revised 1985) were followed.

Reverse-transcription polymerase chain reaction and quantitative real-time polymerase chain reaction

Rats were sacrificed at birth, at the age of 1 week, 1 month, and 3 months (n=4 for each age) under ether anesthesia, and the hearts were removed. Total RNA was extracted from the ventricles using Trizol reagent (Invitrogen), and reverse transcription was performed with 5 μg of RNA from each sample using random primers (Promega) and M-MLV reverse transcriptase (Gibco). To detect the existence of CAR1, CAR2 [9], and splicing variants that were reported in human [31], 35 cycles of polymerase chain reaction (PCR) was performed with cDNA of an adult (3-month-old) rat heart using KOD-Plus (Toyobo). Primers were placed in the V-like domain and in the alternative parts of 3′ terminals of CAR1 and CAR2 (Table 1, Fig. 1A).

Quantitative real-time PCR (qPCR) on LightCycler (Roche) was performed using LightCycler-FirstStart DNA Master SYBR Green I (Roche) as previously described [11]. Primer lists and the scheme of primers for CAR are shown in Table 1 and Fig. 1A. For making standards for quantification, cDNA from the adult rat heart was amplified with each pair of the primers. The products were directly inserted into the pGEM-T vector (Promega) and the recombinant plasmids were isolated after transforming with Escherichia coli JM109 competent cells (Takara) using the MagExtractor plasmid Kit (Toyobo). The plasmids were diluted with DNase free water in a siliconized tube, including 10 ng/ml MS2 RNA (Roche), to prevent adherence to the tube wall, and were used as the standards.

Preparation of antibodies

Polypeptides composing CAR (a: KIYDNYYPDLK in the V-like domain, b: KTQYNQVPSEDFERAPQ in the cytoplasmic domain, and c: PVMIPAQSKDGSIV at C-terminus of CAR1) were chosen to make polyclonal anti-CAR antibodies (Fig. 1A). Anti-CARa antibodies and anti-CARb antibodies were obtained as previously described [13]. Briefly, the polypeptides were synthesized with additional cystein at the C-terminus, conjugated to keyhole limpet hemocyanin (Calbiochem-Novabichem), and used to immunize white rabbits. The resulting antisera were purified by immunoadsorbent affinity chromatography on CNBr-activated Sepharose 4B (Pharmacia) columns coupled with the peptides. Anti-CAR1 C-terminus antibodies (anti-CARc antibodies) were newly prepared to discriminate CAR1 from CAR2. The C terminal polypeptide of CAR1 was conjugated to keyhole limpet hemocyanin (Calbiochem-Novabichem) with glutaraldehyde and used to immunize white rabbits. Purified antibodies were obtained with the same procedures. Monoclonal anti-α smooth muscle actin (αSMA) antibodies (Sigma), monoclonal anti-pan cadherin antibodies (Sigma), and monoclonal anti-connexin43 antibodies (Chemicon International) were purchased.

Sodium dodecyl sulfate-polyacrylamide gel electrophoresis and Western blot analysis

Ventricular tissue of each age group (n=4) was homogenized in cell lysis buffer [20 mmol/l Tris-HCl pH 8.0, 137 mmol/l NaCl, 2 mmol/l ethylene diamine tetraacetic acid (EDTA), 0.3% sodium dodecyl sulfate (SDS), 0.4% sodium deoxycholate, 1 mmol/l phenylmethylsulfonylfluoride (PMSF), and 1% NP-40], rotated at 4°C overnight, and centrifuged at 15,000×g for 30 min. Then, the

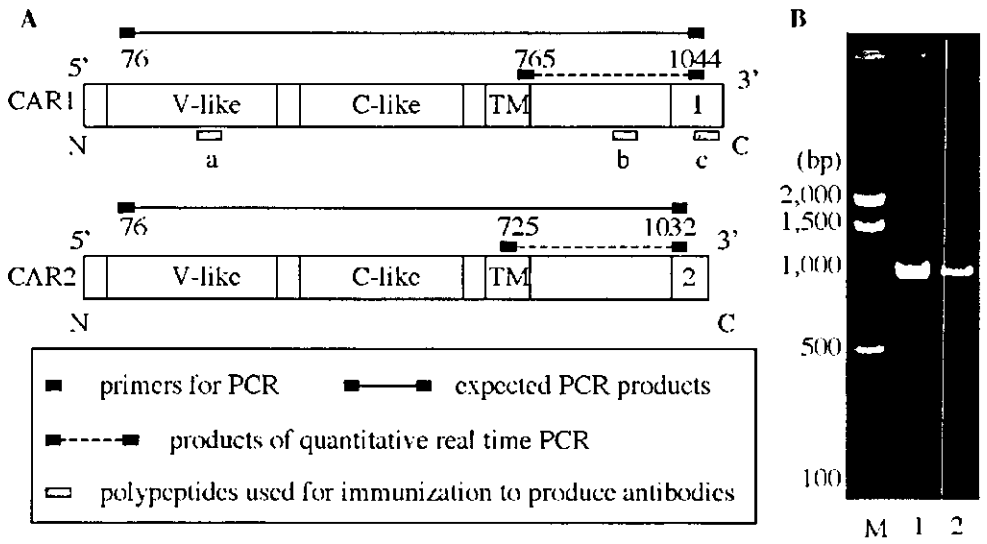

Fig. 1 **A** The design of primers and antibodies. The numbers just beneath or above primers indicate the location in rat coxsackievirus and adenovirus receptor (CAR)1 and CAR2. *V-like* V-like domain. *C-like* C-like domain. *TM* transmembrane domain. *1*, *2* the alternative portions of CAR1 and CAR2. **B** The sizes of polymerase chain reaction products for CAR1 and CAR2 using cDNA from an adult rat heart. A single band was obtained for CAR1 (*1*) and CAR2 (*2*). The sizes were the reasonable and expected ones. *M* size markers

supernatant was stocked at −20°C. After measuring the concentrations of each sample using a DC protein assay kit (Bio-Rad), 10 μg of protein was separated by SDS-polyacrylamide gel electrophoresis (PAGE) (12% acrylamide) and analyzed by immunoblotting with the primary antibodies. Anti-CARa, CARb, and CARc antibodies were diluted to 0.0025 mg/ml, 0.001 mg/ml, and 0.002 mg/ml, respectively. Densitometry was performed for CAR at 46 kDa using computer software (Quantity One, PDI).

Immunohistochemistry and immunofluorescence for tissue samples

The removed hearts of each age group were fixed in Bouin's liquid overnight at 4°C, dehydrated, and embedded in paraffin. Sliced sections (5 micrometers) were prepared on APS coated slides (Matsunami) and deparaffinized. After washing in phosphate-buffered saline (PBS), the slides were heated in 0.01 M citrate buffer (pH 6.0) at 120°C for 20 min in an autoclave, washed three times in PBS, and incubated in methanol containing 0.3% H_2O_2 for neutralizing the endogenous peroxidase. Then, a histofine (R) kit (Nichirei) was diluted with PBS containing 5% skim milk to 1:1 and used for the following procedures. For the detection of CAR, anti-CARc antibodies were chosen based on the results of Western blot analysis to avoid a nonspecific reaction. The antibodies were diluted to 0.002 mg/ml, and normal rabbit immunoglobulin fraction (Dako) was used at the same concentration as the negative control. Visualization was achieved with 3, 3'-diaminobenzidine tetrahydrochloride, and the cell nuclei were counterstained with Mayer's hematoxylin.

Immunofluorescence for CAR was performed using the same methods (without methanol containing 0.3% H_2O_2) until the secondary antibodies, and then, fluorescein isothiocyanate (FITC)-conjugated streptoavidin (Vector, 1/50) was used. Anti-conexin43 antibodies were diluted to 1/500, followed by anti-mouse immunoglobulins labeled with tetramethyl rhodamine isothiocyanate (TRITC) (Dako, 1/50). After the addition of mounting medium (Vector, Vectashield), fluorescent images were obtained using a confocal laser scanning microscope (Fluoview, Olympus).

Primary culture of rat neonatal cardiomyocytes

Cardiomyocytes were prepared from the ventricles of neonatal (3–4 days old) rats by the modified method of Simpson [30]. Briefly, the ventricles were minced and stirred at 37°C in trypsin solution containing 0.1% trypsin (Difco), 0.8% NaCl, 0.04% KCl, 0.1% glucose, and 0.035% $NaHCO_3$. The solution with suspended cells was collected and exchanged every 15 min. The collected solution was added with ice-cold culture medium containing medium199 (Gibco), Ham's F-12 (Gibco), 10% fetal bovine serum (ICN), 0.4% penicillin-streptomycin (Invitrogen), and 0.1 mmol/l 5-bromo-2'-deoxyuridine (Sigma). The suspended cells obtained during the procedures from the second to the seventh cycles were collected by centrifugation at 120×*g*, washed three times with PBS, and resuspended in the culture medium. The cells were cultured for 90 min at 37°C with 5% CO_2 on a flask (Corning), and adherent cells were excluded as fibroblasts. Then, the suspended cells were diluted with the medium at the concentration of 4×10^5 cells/ml and cultured on 6-well cell culture dishes (Iwaki) (1.3×10^3 cells/mm^2) at 37°C with 5% CO_2. The medium was exchanged on day 3.

On days 1, 3, and 7, the wells (n=3) were washed three times with PBS, and only the adherent cells were used as the samples. For preparation of total protein, the wells were agitated with lysis buffer (20 mmol/l Tris-HCl pH 8.0, 137 mmol/l NaCl, 2 mmol/l EDTA, 0.3% SDS, 0.4% sodium deoxycholate, 1 mmol/l PMSF, and 1% NP-40) at room temperature for 10 min and scraped. The contents were rotated at 4°C overnight, and centrifuged at 15,000×*g* for 30 min. Then, the supernatant was stocked at −20°C. For the samples of day 0, the cells suspended prior to starting culturing were used. The cells were washed three times with PBS, and the lysis buffer was added. Total protein was obtained using the same procedures. Then, SDS-PAGE and Western blot analysis were performed as above.

Immunofluorescence for cultured cardiomyocytes

Cardiomyocytes on day 0, prior to starting culturing, were washed three times with PBS, prepared on slides (Matsunami) by Cytospin (Shandon) at 10×*g* for 5 min, and air-dried. For the samples for day 1 and day 2, cardiomyocytes were cultured on collagen I-coated culture slides (Becton Dickinson) at a concentration of 1.1×10^3 cells/mm^2. On day 1 and day 2, the slides were washed three times with PBS, air-dried, and stored at −40°C until the immunofluorescence procedure. The samples were fixed in 4% paraformaldehyde for 20 min, and permeabilized with 0.2% Triton X-100 for 5 min at room temperature. And then, a Histofine (R) kit (Nichirei) was diluted with PBS containing 5% skim milk to 1:1 and used for the following procedures. Anti-CARc antibodies were diluted to 0.002 mg/ml. After washing the secondary antibodies, FITC-conjugated streptoavidin (Vector, 1/50) was used for visualization. Anti-αSMA antibodies, anti-pan cadherin antibodies, and anti-connexin43 antibodies were used at 1/200, 1/500, and 1/500,

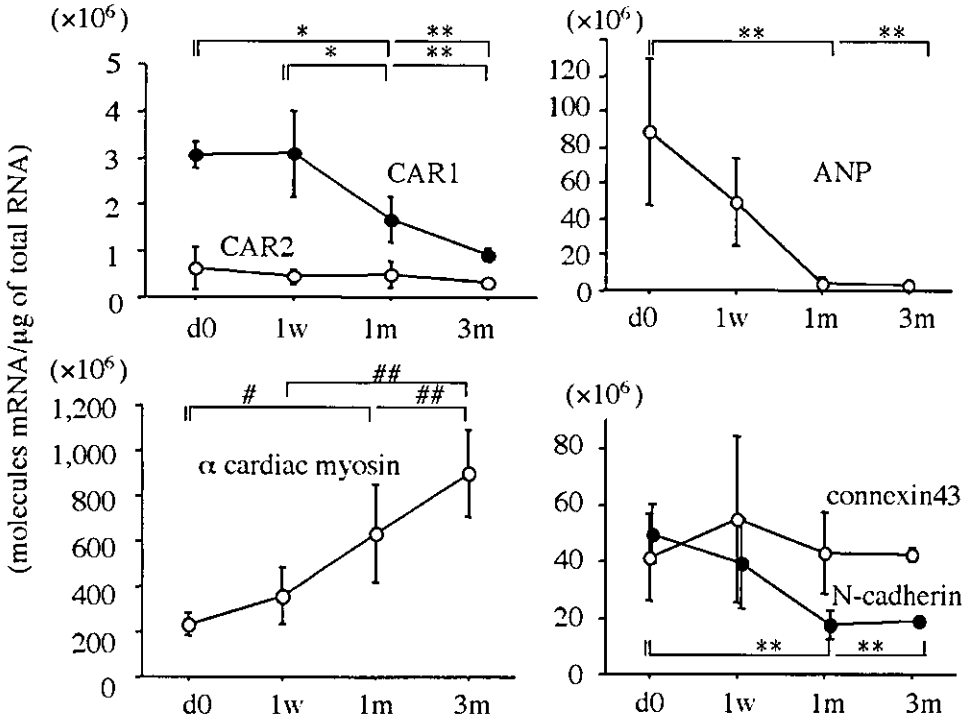

Fig. 2 Expression of cardiac mRNAs during postnatal development. Coxsackievirus and adenovirus receptor (CAR)1 decreased gradually after 1 week, but CAR2 stayed at a lower level. Changes of atrial natriuretic peptide (ANP), α-cardiac myosin, N-cadherin, and conexin43 were also examined as representative mRNAs for fetal phenotypes, adult phenotypes, and intercalated disk molecules. *P<0.05. **P<0.01 by Scheffe test. #P<0.05. ##P<0.01 by the Tukey-Kramer method

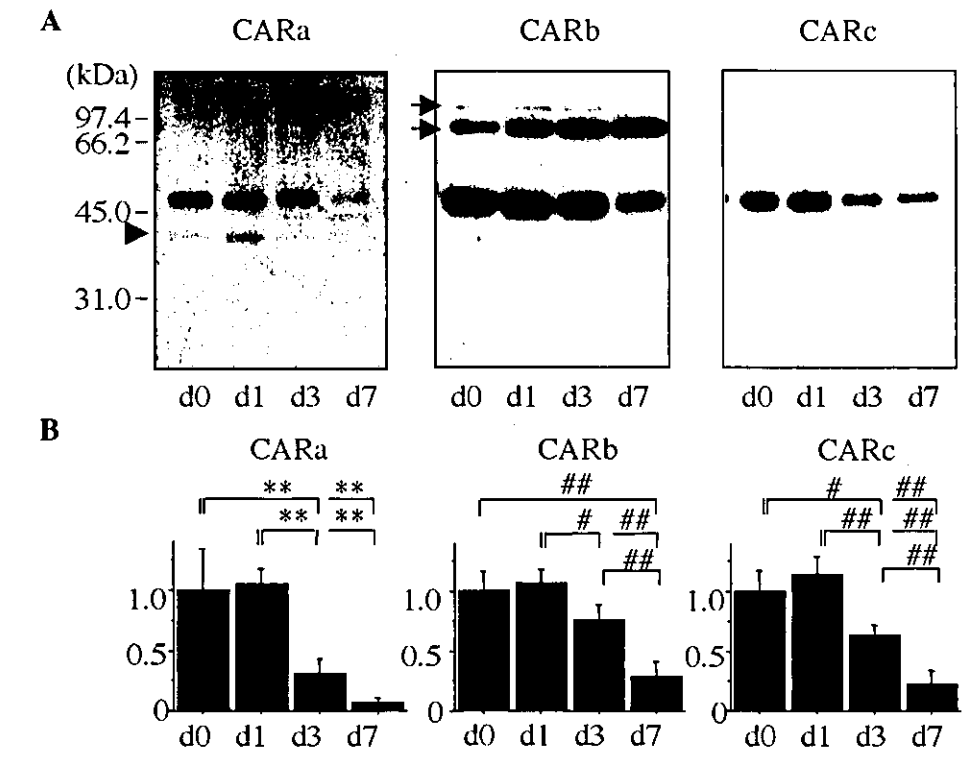

Fig. 3 Expression of coxsackievirus and adenovirus receptor (CAR) and connexin43 proteins during postnatal development. **A** Using three anti-CAR antibodies, CAR was detected at 46 kDa. Anti-CARa and anti-CARb antibodies cross-reacted with other proteins (shown by the *arrowhead* and *arrows*, respectively). Proteins were not identified. Anti-CARc antibodies obviously reacted specifically with CAR. **B** Quantified densitometry. CAR expression relative to day 0 did not change until 1 week after birth. Then, it declined at 1 month and 3 months, and the declines were statistically significant. *P<0.05. **P<0.01 by Scheffe test. #P<0.05. ##P<0.01 by the Tukey-Kramer method

followed by anti-mouse immunoglobulins labeled by TRITC (Dako, 1/50). After the addition of the mounting medium (Vector, VECTASHIELD), fluorescent images were obtained using a confocal laser scanning microscope (Fluoview, Olympus).

Statistical analysis

Values are presented as mean±SD. Statistical analysis was performed by the Tukey-Kramer method, in which SDs of each group were considered equal by the Bartlett test. The Kruskal-Wallis test, followed by the Scheffe test, was used with unequal

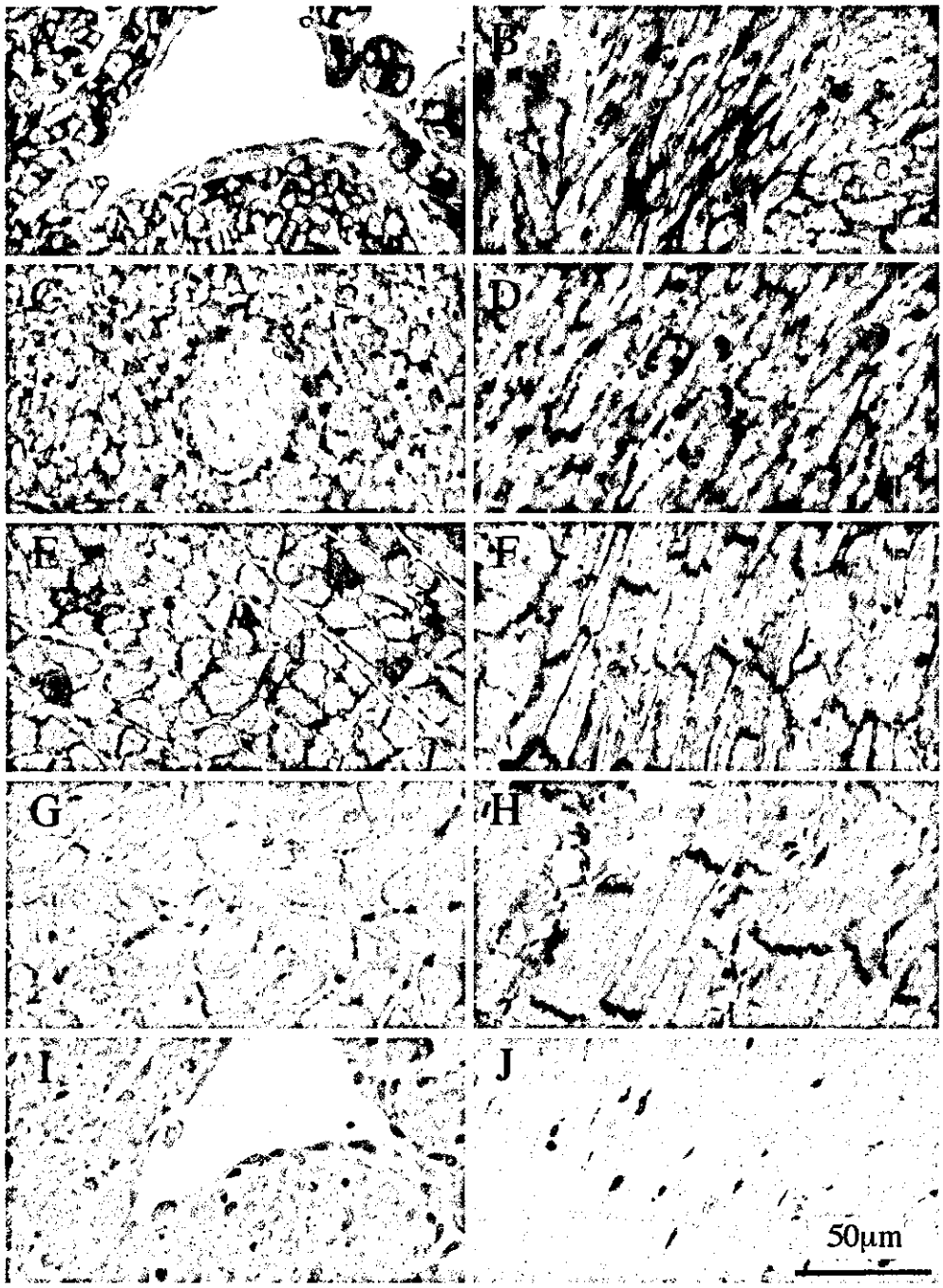

Fig. 4 Imunohistochemistry for coxsackievirus and adenovirus receptor (CAR). The developmental changes in localization of CAR were examined with anti-CARc antibodies. **A, B** At birth. **C, D** 1 week after birth. **E, F** 1 month after birth, **G, H** 3 months after birth. **I, J** Normal rabbit immunoglobulins were used at the same concentration instead of the anti-CARc antibody as the negative controls for **A** and **H**, respectively. The immunoreactivity of CAR is clearly observed on the whole surface of myocytes at birth. Then, CAR seems to localize predominantly at the intercalated disks. It should be noted that the endocardium (**A**) and the vessel walls (**C**) were free of CAR. Original magnifications, ×600

SDs. The difference was considered statistically significant when the P value was less than 0.05.

Results

Expression of mRNA in hearts during postnatal development

The PCR products for CAR1 and CAR2 were detected at expected length, indicating the existence of CAR in adult rat hearts (Fig. 1B). No shorter products, suggesting splicing variants, were detected.

The results of qPCR are shown in Fig. 2. The levels of mRNA of CAR1 were 3.0- to 7.4-fold higher than those of CAR2 throughout the postnatal development. The levels of CAR1 mRNA started to decrease at 1 week after birth. At 1 month of age, the hearts still showed higher levels of CAR1 mRNA ($1.68\pm0.49\times10^6$ molecules mRNA/μg of total RNA) than those at 3 months ($0.91\pm0.14\times10^6$ molecules mRNA/μg of total RNA), although the difference was not statistically significant. However, CAR2 mRNA did not decrease throughout the

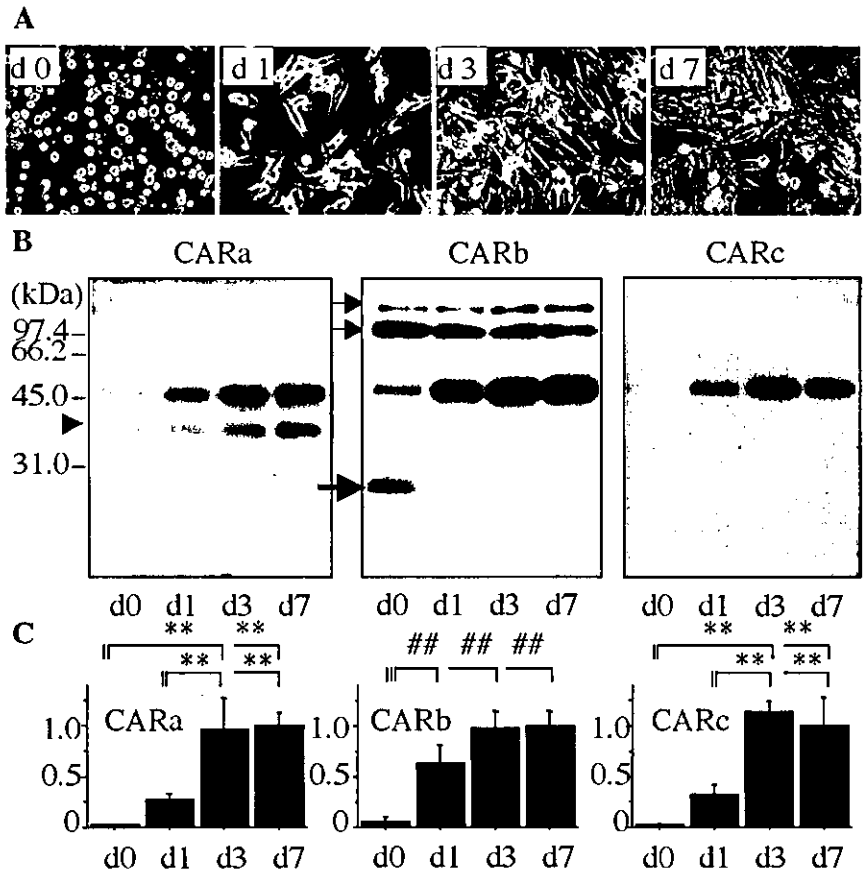

Fig. 5 The culture of cardiomyocytes and expression of coxsackievirus and adenovirus receptor (CAR) protein. **A** Cardiomyocytes were prepared from neonatal rat hearts by trypsin treatment (day 0). Non-adherent cells were removed. From day 0 through day 7, the myocytes grow with increasing intercellular contacts. **B** With three anti-CAR antibodies, CAR was detected at 46 kDa. Anti-CARa antibodies and anti-CARb antibodies cross-reacted with other proteins (*arrowhead* and *thin arrows*, respectively). The smaller band, which detected anti-CARb antibodies (*thick arrow*) was considered to be fragmented CAR. **C** Quantified densitometry. $*P<0.05$. $**P<0.01$ by Scheffe test. $\#P<0.05$. $\#\#P<0.01$ by the Tukey-Kramer method

development and stayed at a lower level. CAR1 decreased to 30% at 3 months after birth, and ANP, a typical fetal phenotype, decreased more remarkably to 2.8%. In contrast, α-cardiac myosin, a typical adult phenotype, increased up to 390% at 3 months. N-cadherin, an adhesion molecule, decreased significantly after 1 week of age, similarly to CAR1, but connexin43 did not change during the development.

Expression of CAR protein in hearts during postnatal development

Using three anti-CAR antibodies, bands of CAR were detected at 46 kDa throughout the development, even at 3 months of age (Fig. 3A). Immunoreactivity of each antibody to CAR showed a difference. The anti-CARa antibody showed weaker band expression than other anti-CAR antibodies. Statistical analysis of the results of densitometry revealed significant decreases of CAR from 1 week to 1 month, and 1 month to 3 months (Fig. 3B).

Immunohistochemistry of hearts

In neonatal rat hearts, CAR was stained on almost the whole surface of cardiomyocytes (Fig. 4A, B). The endocardium of the ventricle or the papillary muscles revealed negative staining for CAR (Fig. 4A). Vessel walls were also negative for CAR (Fig. 4C). After birth, polarity of cardiomyocytes began to emerge, and immunoreactivity of CAR became more clear at the sites of intercalated disks as they grew, while immunoreactivity on the non-contacting surface of cardiomyocytes became fainter (1 week: Fig. 4C, D, 1 month: Fig. 4E, F, 3 months: Fig. 4G, H). In the adult heart, CAR was localized predominantly at the intercalated disks (Fig. 4G, H).

Expression of CAR protein in cultured cardiomyocytes

Figure 5A shows the appearances of cultured cells at different stages. The adhesion of cardiomyocytes to the wells was not complete, even after 24 h of culturing, and the density of adhered cardiomyocytes was low. By day 3, most cells adhered to the wells, and the cell density was similar to that of day 7.

Using three anti-CAR antibodies, the bands of CAR were detected at 46 kDa (Fig. 5B). On day 0, cardiomyocytes had lost most of the CAR molecules after treatment in a trypsin solution. The result indicated that most CAR molecules in neonatal rat hearts had existed on the surface of the cells and were digested by trypsin. On day 1, the blot for CAR became apparent, using all three antibodies, although a significant rise was confirmed only

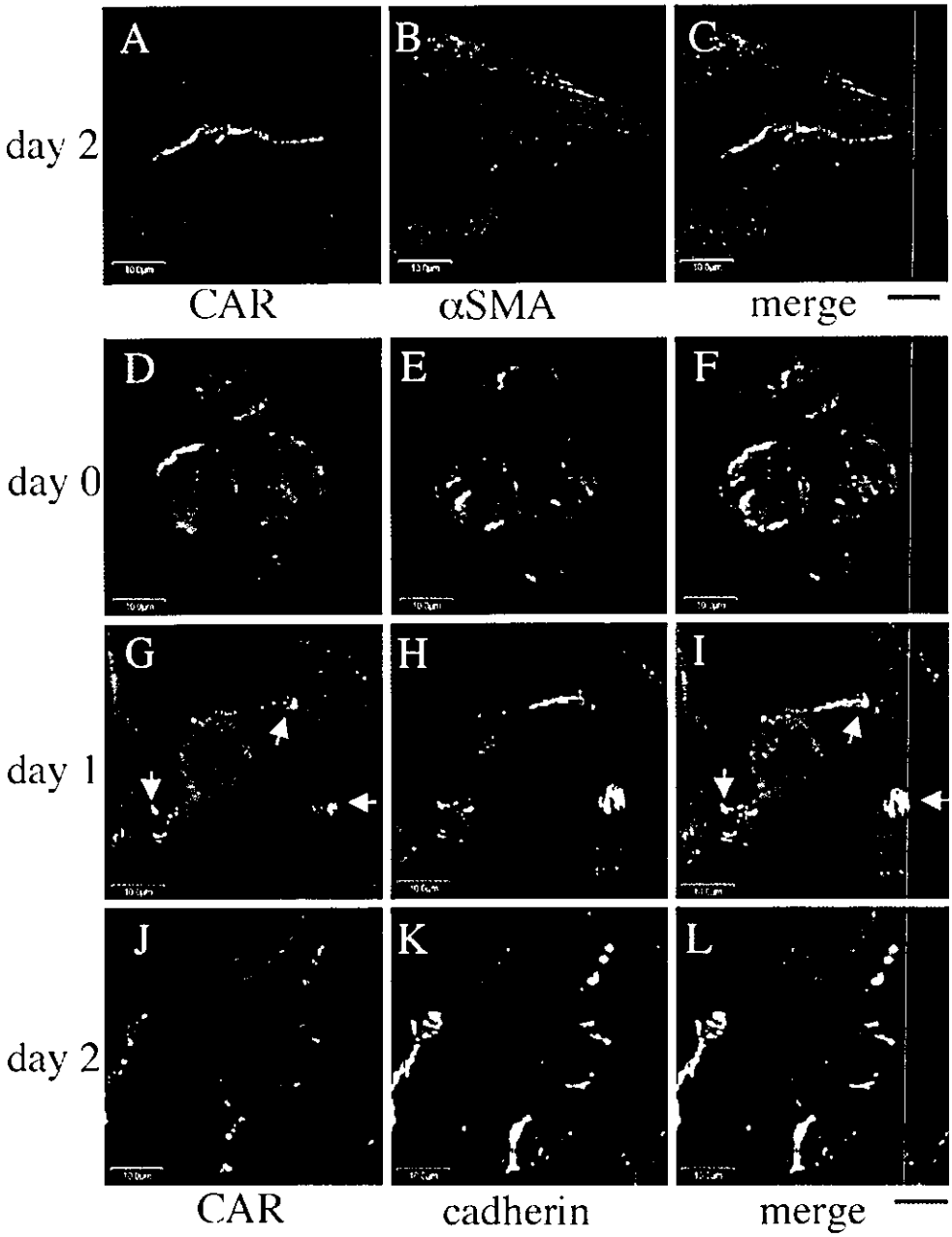

Fig. 6 Immunofluorescence of cultured cardiomyocytes for coxsackievirus and adenovirus receptor (CAR) and cadherin. **A, B, C** After 2 days of culturing, CAR labeled green with fluorescein isothiocyanate (FITC) localizes along the junction between the two cardiomyocytes, as identified by anti-α smooth muscle actin antibody, labeled red by tetramethyl rhodamine isothiocyanate (TRITC). **D, E, F, G, H, I, J, K, L** The localization of CAR, labeled green with FITC, was compared with cadherin, labeled red by TRITC. **D, E, F** The cardiomyocytes on day 0 have lost CAR on the cell surface due to trypsin treatment. Cadherin remains stainable on the cell surface. **G, H, I** On day 1, CAR starts to localize at the sites of cellular contacts (*arrows*), where cadherin is also stained. **J, K.** On day 2, co-localization of CAR and cadherin is obvious along the junctions. Original magnifications, ×600. Scale bars, 10 μm

for CARb (Fig. 5C). The expression of CAR reached a plateau by day 3 and remained stable until day 7.

Immunofluorescence of cultured cardiomyocytes

Neonatal cardiomyocytes were specified by anti-αSMA antibodies. CAR was clearly confined to the sites of intercellular contact of cardiomyocytes (Fig. 6A, B, C). After trypsin treatment on day 0, CAR did not exist on the cell surface and was stained differently than cadherin (Fig. 6D, E, F). Soon after the establishment of cellular contacts on day 1, CAR was localized to the site of intercellular contacts (Fig. 6G, I *arrow*), and cadherin was observed at the same site (Fig. 6H, I). By day 2, CAR was found at the sites of intercellular contact in parallel with cadherin (Fig. 6J, K, L).

Localization of CAR and connexin43 in vivo and in vitro

CAR was shown on the whole surface of cardiomyocytes in vivo at birth. Connexin43 was only sparsely stained, but a polarity was not found (Fig. 7A, B, C). In contrast, at 3 months of age, both CAR and connexin43 showed apparent polarity and were co-localized predominantly at the intercalated disks (Fig. 7D, E, F).

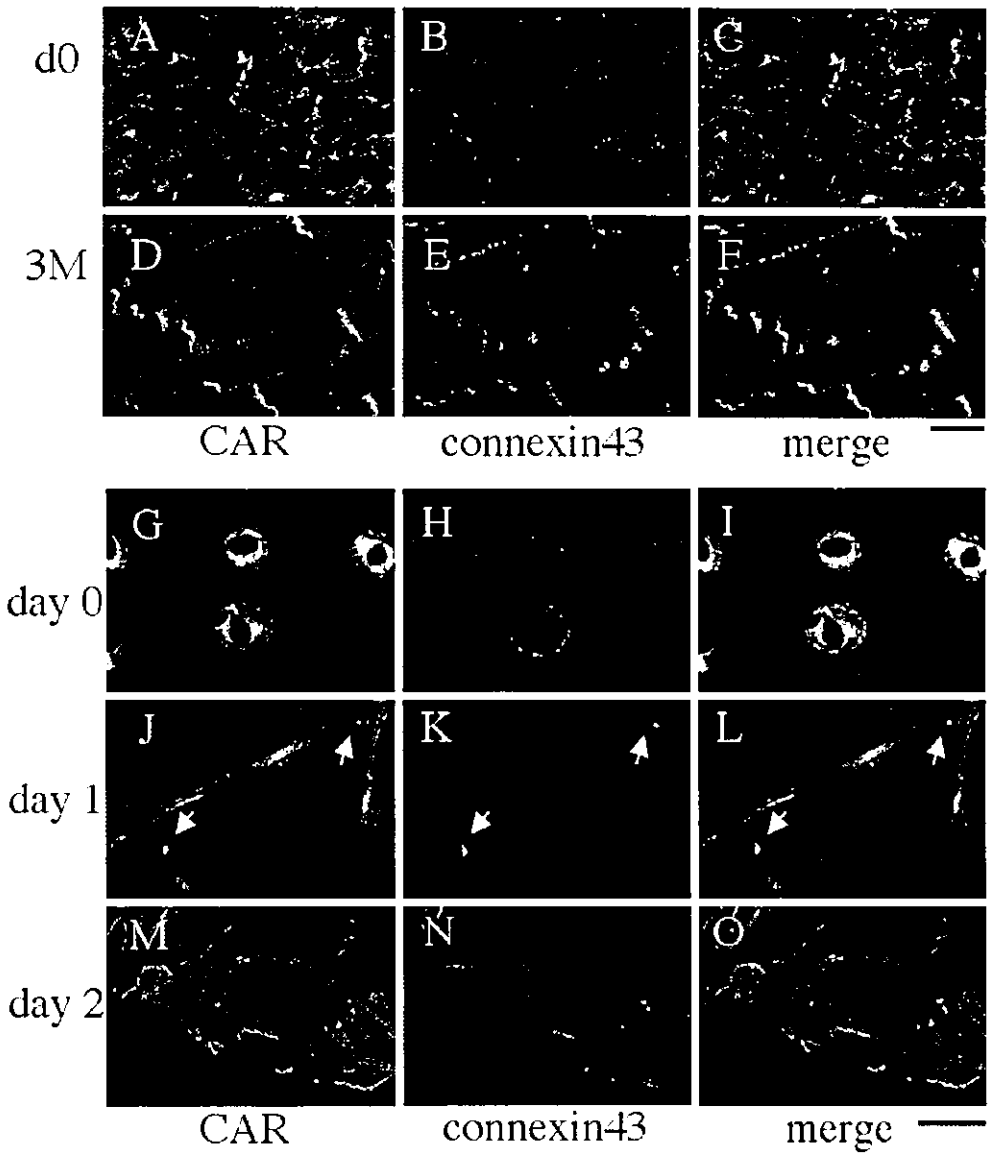

Fig. 7 The localizations of coxsackievirus and adenovirus receptor (CAR) and conexin43 in rat hearts and in cultured cardiomyocytes. **A, B, C** In newborn rat hearts, CAR, labeled green with fluorescein isothiocyanate (FITC), localizes on almost the whole surface of cardiomyocytes. Connexin43 is only sparsely stained but a polarity is not found. **D, E, F.** In the adult rat heart, CAR localizes predominantly at the intercalated disks co-localizing with connexin43. **G, H, I** Trypsin-treated cardiomyocytes have lost CAR from the cell surface, and connexin43 sparsely remains. **J, K, L** On day 1, CAR and connexin43 are co-localized at the sites of cellular contacts (*arrows*). **M, N, O** On day 2, CAR and connexin43 are co-localized along the intercellular junctions between the cells. Original magnifications, ×600. Scale bar, 20 μm

In suspended neonatal cardiomyocytes, connexin43 was stained mainly beneath the cell surface, even after trypsin treatment (Fig. 7H, I). On day 1, CAR and connexin43 were shown to coexist at the sites of cell–cell contact (Fig. 7J, K, L *arrow*). By day 2, the sites of intercellular contacts became linear, and CAR and connexin43 existed together as dense lines along the junctions (Fig. 7M, N, O).

Discussion

The localization of CAR was emphasized as the determinant of coxsackievirus and adenovirus infection [6, 9, 25, 33, 34, 35], and this is the first study demonstrating spatiotemporal change of CAR in the heart during postnatal development. The results will explain the susceptibility of neonates and children to viral myocarditis.

In this study, we confirmed the postnatal decrease of cardiac CAR prior to histological examinations. As demonstrated in a previous report [10], the postnatal decrease of CAR mRNA in the heart was confirmed, but in this study, we found that a decline of the mRNA level was associated with a decline of CAR protein. Decreases of CAR expression in adults have already been reported in the skeletal muscle [19], brain [13], and heart [10, 14] of rodents. The decline of cardiac CAR seemed less remarkable and slower than those of skeletal muscle and brain. The presence of a considerable amount of CAR suggested that CAR has some roles in the heart, even in adults. CAR is a molecule belonging to the immunoglobulin superfamily, and we reported its role in homophilic cell–cell contact [13]. It was interesting that the developmental decrease of an adhesion molecule, N-cadherin,

was similar to that of CAR, at least with respect to mRNA, but the developmental change of connexin43, which is a type of channel protein on the intercalated disk, was not. We did not focus on the physiological function of CAR in this study, and the role of CAR in the heart remains to be studied.

Our principal finding was the spatiotemporal change of CAR during postnatal development, and it was determined using anti-CAR antibodies. First, we prepared three anti-CAR antibodies, anti-CARa, anti-CARb, and anti-CARc, to precisely determine the change of localization of CAR and then, tested their specificity. In Western blot analysis, both anti-CARa and CARb antibodies showed additional bands, which were considered to be fragments of CAR or unrelated unknown molecules. Anti-CARc antibody reacted only with CAR1 and showed no additional bands; this is the reason that anti-CARc antibody was used in the histological studies. We also performed immunohistochemistry with anti-CARb antibody to detect both CAR1 and CAR2 and confirmed the same staining pattern in developing hearts (data not shown); at birth, CAR was found diffusely on the surface of myocytes, but was localized predominantly at the site of intercellular contacts in the adult heart.

However, in cultured cardiomyocytes, the cells revealed diffuse immunoreactivity to the anti-CARc antibody, which was strongest on day 0. At that time, Western blot analysis showed almost a negative band at 46 kDa. This would mean that during the preparation of cardiomyocytes, the extracellular domains of CAR must be digested by trypsin, and fragmented CAR in the cytoplasma would be stained or the immunoreactivity might be non-specific. The size of the smaller molecule detected by anti-CARb antibody on day 0 was identical to that of the proteolysed CAR in trypsin-treated HeLa cells [4], and the reason for the absence of the shorter band with anti-CARc antibody was unknown. Nevertheless, CAR was clearly accumulated at the site of the contact once the cultured myocytes established intercellular contact and increased with intercellular contacts.

Interestingly, it was only when cardiomyocytes were in immature hearts that cardiomyocytes expressed CAR and other intercalated disk proteins onto the whole surface without polarity. Reported localizations of intercalated disk proteins, N-cadherin, and connexin43 in vivo [1, 24, 28] and in vitro [23, 28] supported our results and were similar to that of CAR in terms of polarity. The localizations seemed to depend upon the environment, and, thus, there must be factors that lead those molecules, including CAR, to the whole surface of cardiomyocytes without polarity in the immature heart. The spatiotemporal change of CAR was considered to be a part of the dynamic movement of molecules during the maturation of the intercalated disk.

Since CAR acts as a common receptor for both coxsackievirus and adenovirus and the viruses are frequent causes of myocarditis in humans, the up-regulation in the hearts and the change of the intracellular localization of CAR during development may affect the susceptibility to these viruses. Actually, newborn and young children are the most affected. When CAR is localized on the whole cell surface, viral infection occurs more easily, as shown in airway epithelial cells [25, 34]. However, when CAR is exclusively localized at the site of cell–cell contact, the intercalated disks, viruses might be unable to use the receptor to infect the heart, and this can partly explain why viral myocarditis is common in neonates and young children.

In conclusion, CAR was expressed abundantly on the whole surface of cardiomyocytes in immature rat hearts. Not only the expression level, but also the localization of CAR, are the possible determinants of the susceptibility of neonates and children to viral myocarditis. Further studies will be needed to clarify the physiological and pathological role of CAR in the heart and may possibly lead to prevention or treatment of viral myocarditis and dilated cardiomyopathy.

Acknowledgement This study was supported in part by a grant for research on specific diseases from the Ministry of Health, Labor and Welfare.

References

1. Angst BD, Khan LU, Severs NJ, Whitely K, Rothery S, Thompson RP, Magee AI, Gourdie RG (1997) Dissociated spatial patterning of gap junctions and cell adhesion junctions during postnatal differentiation of ventricular myocardium. Circ Res 80:88–94
2. Bergelson JM, Cunningham JA, Droguett G, Kurt-Jones EA, Krithivas A, Hong JS, Horwitz MS, Crowell RL, Finberg RW (1997) Isolation of a common receptor for coxsackie B viruses and adenoviruses 2 and 5. Science 275:1320–1323
3. Bowles NE, Towbin JA (2003) Childhood myocarditis and dilated cardiomyopathy. In: Cooper LT (ed) Myocarditis: from bench to bedside. Humana Press, Totowa, pp 559–587
4. Carson SD (2000) Limited proteolysis of the coxsackievirus and adenovirus receptor (CAR) on HeLa cells exposed to trypsin. FEBS Lett 484:149–152
5. Carson SD, Chapman NN, Tracy SM (1997) Purification of the putative coxsackievirus B receptor from HeLa cells. Biochem Biophys Res Commun 233:325–328
6. Cohen CJ, Shieh JT, Pickles RJ, Okegawa T, Hsieh JT, Bergelson JM (2001) The coxsackievirus and adenovirus receptor is a transmembrane component of the tight junction. Proc Natl Acad Sci U S A 98:15191–15196
7. Dec GW, Fuster V (1994) Idiopathic dilated cardiomyopathy. N Engl J Med 331:1564–1575
8. Douglas JT, Kim M, Sumerel LA, Carey DE, Curiel DT (2001) Efficient oncolysis by a replicating adenovirus (ad) in vivo is critically dependent on tumor expression of primary ad receptors. Cancer Res 61:813–917
9. Fechner H, Haack A, Wang H, Wang X, Eizema K, Pauschinger M, Schoemaker R, Veghel R, Houtsmuller A, Schultheiss HP, Lamers J, Poller W (1999) Expression of coxsackie adenovirus receptor and alpha-integrin does not correlate with adenovector targeting in vivo indicating anatomical vector barriers. Gene Ther 6:1520–1535
10. Fechner H, Noutsias M, Tschoepe C, Hinze K, Wang X, Escher F, Pauschinger M, Dekkers D, Vetter R, Paul M, Lamers J, Schultheiss HP, Poller W (2003) Induction of coxsackievirus-adenovirus-receptor expression during myocardial tissue formation and remodeling: identification of a cell-to-cell contact-dependent regulatory mechanism. Circulation 107:876–882

11. Hanawa H, Abe S, Hayashi M, Yoshida T, Yoshida K, Shiono T, Fuse K, Ito M, Tachikawa H, Kashimura T, Okura Y, Kato K, Kodama M, Maruyama S, Yamamoto T, Aizawa Y (2002) Time course of gene expression in rat experimental autoimmune myocarditis. Clin Sci 103:623–632
12. Hirschman SZ, Hammer GS. Coxsackie virus myopericarditis. A microbiological and clinical review. Am J Cardiol 34:224–232
13. Honda T, Saitoh H, Masuko M, Katagiri-Abe T, Tominaga K, Kozakai I, Kobayashi K, Kumanishi T, Watanabe YG, Odani S, Kuwano R (2000) The coxsackievirus-adenovirus receptor protein as a cell adhesion molecule in the developing mouse brain. Brain Res Mol Brain Res 77:19–28
14. Ito M, Kodama M, Masuko M, Yamaura M, Fuse K, Uesugi Y, Hirono S, Okura Y, Kato K, Hotta Y, Honda T, Kuwano R, Aizawa Y (2000) Expression of coxsackievirus and adenovirus receptor in hearts of rats with experimental autoimmune myocarditis. Circ Res 86:275–280
15. Leon RP, Hedlund T, Meech SJ, Li S, Schaack J, Hunger SP, Duke RC, DeGregori J (1998) Adenoviral-mediated gene transfer in lymphocytes. Proc Natl Acad Sci U S A 95:13159–13164
16. Martin AB, Webber S, Fricker FJ, Jaffe R, Demmler G, Kearney D, Zhang YH, Bodurtha J, Gelb B, Ni J, Bricker TB, Towbin JA (1994) Acute myocarditis. Rapid diagnosis by PCR in children. Circulation 90:330–339
17. Montague TJ, Lopaschuk GD, Davies NJ (1990) Viral heart disease. Chest 98:190–199
18. Nakagawa M, Sato A, Okagawa H, Kondo M, Okuno M, Takamatsu T (1999) Detection and evaluation of asymptomatic myocarditis in schoolchildren: report of four cases. Chest 116:340–345
19. Nalbantoglu J, Pari G, Karpati G, Holland PC (1999) Expression of the primary coxsackie and adenovirus receptor is downregulated during skeletal muscle maturation and limits the efficacy of adenovirus-mediated gene delivery to muscle cells. Hum Gene Ther 10:1009–1019
20. Nalbantoglu J, Larochelle N, Wolf E, Karpati G, Lochmuller H, Holland PC (2001) Muscle-specific overexpression of the adenovirus primary receptor CAR overcomes low efficiency of gene transfer to mature skeletal muscle. J Virol 75:4276-4282
21. Nicholson F, Ajetunmobi JF, Li M, Shackleton EA, Starkey WG, Illavia SJ, Muir P, Banatvala JE (1995) Molecular detection and serotypic analysis of enterovirus RNA in archival specimens from patients with acute myocarditis. Br Heart J 74:522–527
22. Noutsias M, Fechner H, de Jonge H, Wang X, Dekkers D, Houtsmuller AB, Pauschinger M, Bergelson J, Warraich R, Yacoub M, Hetzer R, Lamers J, Schultheiss HP, Poller W (2001) Human coxsackie-adenovirus receptor is colocalized with integrins alpha(v)beta(3) and alpha(v)beta(5) on the cardiomyocyte sarcolemma and upregulated in dilated cardiomyopathy: implications for cardiotropic viral infections. Circulation 104:275–280
23. Oyamada M, Kimura H, Oyamada Y, Miyamoto A, Ohshika H, Mori M (1994) The expression, phosphorylation, and localization of connexin 43 and gap-junctional intercellular communication during the establishment of a synchronized contraction of cultured neonatal rat cardiac myocytes. Exp Cell Res 212:351–358
24. Peters NS, Severs NJ, Rothery SM, Lincoln C, Yacoub MH, Green CR (1994) Spatiotemporal relation between gap junctions and fascia adherens junctions during postnatal development of human ventricular myocardium. Circulation 90:713–725
25. Pickles RJ, Fahrner JA, Petrella JM, Boucher RC, Bergelson JM (2000) Retargeting the coxsackievirus and adenovirus receptor to the apical surface of polarized epithelial cells reveals the glycocalyx as a barrier to adenovirus-mediated gene transfer. J Virol 74:6050–6057
26. Pisani B, Taylor DO, Mason JW (1997) Inflammatory myocardial diseases and cardiomyopathies. Am J Med 102:459–469
27. Poller W, Fechner H, Noutsias M, Tschoepe C, Schultheiss HP (2002) Highly variable expression of virus receptors in the human cardiovascular system Implications for cardiotropic viral infections and gene therapy. Z Kardiol 91:978–991
28. Reinecke H, Zhang M, Bartosek T, Murry CE (1999) Survival, integration, and differentiation of cardiomyocyte grafts: a study in normal and injured rat hearts. Circulation 100:193–202
29. Rosenberg HS, McNamara DG (1964) Acute myocarditis in infancy and childhood. Prog Cardiovasc Dis 7:179–197
30. Simpson P, Savion S (1982) Differentiation of rat myocytes in single cell cultures with and without proliferating nonmyocardial cells. Cross-striations, ultrastructure, and chronotropic response to isoproterenol. Circ Res 50:101–116
31. Thoelen I, Magnusson C, Tagerud S, Polacek C, Lindberg M, Van Ranst M (2001) Identification of alternative splice products encoded by the human coxsackie-adenovirus receptor gene. Biochem Biophys Res Commun 287:216–222
32. Tomko RP, Xu R, Philipson L (1997) HCAR and MCAR: the human and mouse cellular receptors for subgroup C adenoviruses and group B coxsackieviruses. Proc Natl Acad Sci U S A 94:3352–3356
33. Walters RW, Grunst T, Bergelson JM, Finberg RW, Welsh MJ, Zabner J (1999) Basolateral localization of fiber receptors limits adenovirus infection from the apical surface of airway epithelia. J Biol Chem 274:10219–10226
34. Walters RW, van't Hof W, Yi SM, Schroth MK, Zabner J, Crystal RG, Welsh MJ (2001) Apical localization of the coxsackie-adenovirus receptor by glycosyl-phosphatidylinositol modification is sufficient for adenovirus-mediated gene transfer through the apical surface of human airway epithelia. J Virol 75:7703–7711
35. Walters RW, Freimuth P, Moninger TO, Ganske I, Zabner J, Welsh MJ (2002) Adenovirus fiber disrupts CAR-mediated intercellular adhesion allowing virus escape. Cell 110:789–799
36. Wan YY, Leon RP, Marks R, Cham CM, Schaack J, Gajewski TF, DeGregori J (2000) Transgenic expression of the coxsackie/adenovirus receptor enables adenoviral-mediated gene delivery in naive T cells. Proc Natl Acad Sci U S A 97:13784–13789
37. Young JAT (2001) Virus entry and uncoating. In: Kimpe DM, Howley PM (eds) Fieles virology. Lippincott Williams & Wilkins, Philadelphia, pp 87–103

循環器病の診断と治療に関するガイドライン（2001－2002年度合同研究班報告）

川崎病心臓血管後遺症の診断と治療に関するガイドライン

Guidelines for diagnosis and management of cardiovascular sequelae in Kawasaki disease (JCS 2003)

合同研究班参加学会：日本循環器学会，日本心臓病学会，日本小児科学会，日本小児循環器学会，日本胸部外科学会

班　長　原　田　研　介　日本大学小児科

ｱﾄﾞﾊﾞｲｻﾞｰ　加　藤　裕　久　久留米大学循環器病研究所

班　員　赤　木　禎　治　久留米大学小児科

　　唐　澤　賢　祐　日本大学小児科

　　北　村　惣一郎　国立循環器病センター

　　佐　地　　勉　東邦大学第一小児科

　　鈴　木　淳　子　東京逓信病院小児科

　　馬　場　　清　倉敷中央病院小児科

班　員　藤　原　久　義　岐阜大学第二内科

協力員　鮎　沢　　衛　日本大学小児科

　　岡　田　知　雄　日本大学小児科

　　小　川　俊　一　日本医科大学小児科

　　荻　野　廣太郎　関西医科大学小児科

　　西　垣　和　彦　岐阜大学第二内科

外部評価委員

　　遠　藤　真　弘　東京女子医科大学日本心臓血圧研究所外科

　　尾　内　善四郎　島津製作所附属島津診療所内科

　　中　澤　　誠　東京女子医科大学日本心臓血圧研究所循環器小児科

　　山　口　　徹　虎の門病院

Circulation Journal

Vol. 67 Supplement Ⅳ

(Pages 1111-1174)

循環器病の診断と治療に関するガイドライン（2001－2002年度合同研究班報告）

川崎病心臓血管後遺症の診断と治療に関するガイドライン

Guidelines for diagnosis and management of cardiovascular sequelae in Kawasaki disease (JCS 2003)

合同研究班参加学会：日本循環器学会，日本心臓病学会，日本小児科学会，日本小児循環器学会，日本胸部外科学会

班　長　原田研介　日本大学小児科

ｱﾄﾞﾊﾞｲｻﾞｰ　加藤裕久　久留米大学循環器病研究所

班　員　赤木禎治　久留米大学小児科
唐澤賢祐　日本大学小児科
北村惣一郎　国立循環器病センター
佐地勉　東邦大学第一小児科
鈴木淳子　東京逓信病院小児科
馬場清　倉敷中央病院小児科

班　員　藤原久義　岐阜大学第二内科

協力員　鮎沢衛　日本大学小児科
岡田知雄　日本大学小児科
小川俊一　日本医科大学小児科
荻野廣太郎　関西医科大学小児科
西垣和彦　岐阜大学第二内科

外部評価委員

遠藤真弘　東京女子医科大学日本心臓血圧研究所外科
尾内善四郎　島津製作所附属島津診療所内科
中澤誠　東京女子医科大学日本心臓血圧研究所循環器小児科
山口徹　虎の門病院

目　次

Ⅰ　序文：背景，ガイドラインの作成にあたって
Ⅱ　心臓後遺症の病理・病態と自然歴
1. 冠動脈障害
2. 心筋障害
3. 弁膜障害
4. 動脈硬化
Ⅲ　診　断
1. 血液検査
1）心筋梗塞
2）動脈硬化
2. 生理検査
1）安静時心電図
2）運動負荷心電図
3）ホルター心電図
4）加算平均心電図
5）体表面電位図・薬剤負荷心電図・心磁図
3. 画像診断
1）胸部X線写真
2）心エコー検査
3）核医学検査
4）その他の画像診断法
5）画像診断法の選択
4. 心臓カテーテル検査
1）冠動脈造影
2）心機能検査
3）血管内超音波法
4）冠動脈狭窄の機能的重症度評価
Ⅳ　治療法
1. 薬物療法
1）治療方針
2）虚血発作の治療
3）薬物療法
2. 非薬物療法
1）冠動脈インターベンション
2）冠動脈バイパス手術
3）その他の手術
3. 急性心筋梗塞に対する初期（内科的）治療
4. 生活・運動指導
Ⅴ　経過観察
Ⅵ　成人期の対応，循環器内科医との連携
Ⅶ　まとめ
Ⅷ　文　献

本ガイドラインで用いられる主な略語

ACC：American College of Cardiology
ACE：angiotensin converting enzyme
AHA：American Heart Association
AN：Aneurysm
ARB：Angiotensin receptor blocker
ATP：adenosine triphosphate
BMIPP：betamethyl-ioophenyl-pentadecanoic acid
CABG：coronary artery bypass grafting
CFR：coronary flow reserve
CK：creatine kinase
CT：computed tomography
EF：ejection fraction
FFRmyo：Myocardial fractional flow reserve
FS：fraction shortening
Ga：Gallium
H-FABP：heart-type fatty acid-binding protein
HDL：high-density lipoprotein
ICT：intracoronary thrombolysis
ISDN：isosorbide dinitrate
IVUS：intravascular ultrasound
LDL：low-density lipoprotein
MIBG：metaiodobenzylguanidine
MLC：myosin light chain
MRA：Magnetic resonance angiography
MRI：Magnetic resonance imaging
PCI：percutaneous coronary intervention
PDE：phosphodiesterase
PET：Positron emission tomography
POBA：plain old balloon angioplasty
SPECT：Single photon emission computed tomography
Tc：Tecnechium
Tl：Thallium
TnT：troponin T
t-PA：tissue plasminogen activator

I 序 文

初めて川崎病が報告された1967年[1]から，35年以上が経過した．川崎病既往者の多くの症例が内科領域の年齢に到達している．川崎病は，世界中で多くの研究がされ，その原因論，心臓血管後遺症に関する多数の報告がある．原因に関しては残念ながら明らかにされていないが，心臓血管後遺症に関しては，詳細な研究が行われ，病態，自然歴，診断，および治療においては，確立されたものがある．そこで，日本循環器学会としてガイドラインを作成することになった．現在までに旧厚生省厚生科学研究で行った川崎病冠動脈後遺症に対するカテーテル治療に関するガイドライン，米国およびカナダのガイドライン，および日本川崎病研究会運営委員会編：川崎病の管理基準（2002年改訂）[2]などがある．しかし，循環器医を対象とした心臓血管後遺症全般にわたる詳細なガイドラインはない．従って，対象が最も多い本邦で現時点での心臓血管後遺症に関するガイドラインをまとめることは小児循環器医から循環器内科医への連携を確立するために重要なものと思う．

表1に，現在，2002年に改訂された川崎病診断の手引きを示す[3]．川崎病急性期はこの診断の手引きで診断する．成人例で川崎病既往が不明で，冠動脈瘤の形態から川崎病が疑われる場合には，病歴からこの診断の手引きが手がかりになるであろう．今回，川崎病心臓血管後遺症のガイドラインを作成するにあたって，まず，協議されたた点は，冠動脈瘤の大きさの基準および重症度評価を統一した基準で分類することであった．よって，表2は，過去の分類および専門医の見解から本ガイドラインとしての基準として合意事項とした．

ガイドライン作成にあたっては，引用文献の証拠のレベルはAHA/ACCのガイドライン形式を踏襲した．過去に報告された川崎病および本ガイドライン関連の研究論文を集約し証拠のレベルを表3のように行い，引用文献の項に記載した．川崎病研究論文に関しては，症例報告の積み重ねが現在の臨床評価につながっていることから，症例報告も重要視した．また，多施設の研究がほとんどされていない現状を考慮し，班員の意見交換から導いた見解もガイドラインとして採用した．勧告が可能な診断法および治療法については，表4の勧告の程度を用いた．

ガイドラインの構成については，川崎病心臓血管後遺症の時期から対象を分類すると，急性期（30病日以内），小児期—遠隔期，成人期—遠隔期になり，このガイドラインでは主に小児期から成人期の遠隔期を対象に構成した．しかし，項目によっては，両者に関わる点から，小児期または成人期に比重を置いた項があり，その点は各項に対象を明記する形とした．

表1 川崎病（MCLS，小児急性熱性皮膚粘膜リンパ節症候群）診断の手引き

本症は，主として4歳以下の乳幼児に好発する原因不明の疾患で，その症候は以下の主要症状と参考条項とに分けられる．

A 主要症状

1. 5日以上続く発熱（ただし，治療により5日未満で解熱した場合も含む）
2. 両側眼球結膜の充血
3. 口唇，口腔所見：口唇の紅潮，いちご舌，口腔咽頭粘膜のびまん性発赤
4. 不定形発疹
5. 四肢末端の変化：（急性期）手足の硬性浮腫，掌蹠ないしは指趾先端の紅斑☆（回復期）指先からの膜様落屑
6. 急性期における非化膿性頸部リンパ節腫脹

6つの主要症状のうち5つ以上の症状を伴うものを本症とする．

ただし，上記6主要症状のうち，4つの症状しか認められなくても，経過中に断層心エコー法もしくは，心血管造影法で，冠動脈瘤（いわゆる拡大を含む）が確認され，他の疾患が除外されれば本症とする．

B 参考条項

以下の症候および所見は，本症の臨床上，留意すべきものである．

1. 心血管：聴診所見（心雑音，奔馬調律，微弱心音），心電図の変化（PR・QTの延長，異常Q波，低電位差，ST-Tの変化，不整脈），胸部X線所見（心陰影拡大），断層心エコー図所見（心膜液貯留，冠動脈瘤），狭心症状，末梢動脈瘤（腋窩など）
2. 消化器：下痢，嘔吐，腹痛，胆嚢腫大，麻痺性イレウス，軽度の黄疸，血清トランスアミナーゼ値上昇
3. 血液：核左方移動を伴う白血球増多，血小板増多，赤沈値の促進，CRP陽性，低アルブミン血症，$\alpha 2$ グロブリンの増加，軽度の貧血
4. 尿：蛋白尿，沈査の白血球増多
5. 皮膚：BCG接種部位の発赤・痂皮形成，小膿疱，爪の横溝
6. 呼吸器：咳嗽，鼻汁，肺野の異常陰影
7. 関節：疼痛，腫脹
8. 神経：髄液の単核球増多，けいれん，意識障害，顔面神経麻痺，四肢麻痺

備考

1. 主要症状Aの5は，回復期所見が重要視される．
2. 急性期における非化膿性頸部リンパ節腫脹は他の主要症状に比べて発現頻度が低い（約65％）
3. 本症の性比は，1.3～1.5：1で男児に多く，年齢分布は4歳以下が80～85％を占め，致命率は0.1％前後である．
4. 再発例は2～3％に，同胞例は1～2％にみられる．
5. 主要症状を満たさなくても，他の疾患が否定され，本症が疑われる容疑例が約10％存在する．この中には冠動脈瘤（いわゆる拡大を含む）が確認される例がある．

（厚生労働省川崎病研究班作成改訂5版）

表2 川崎病心臓血管病変の重症度分類

(a) 急性期冠動脈瘤の分類

小動脈瘤（ANs）または拡大（Dil）：内径4 mm以下の局所性拡大所見を有するもの．
年長児（5歳以上）で周辺冠動脈内径の1.5倍未満のもの．

中等瘤（ANm）：4 mm < 内径 ≤ 8 mm
年長児（5歳以上）で周辺冠動脈内径の1.5倍から4倍のもの．

巨大瘤（ANl）：8 mm < 内径
年長児（5歳以上）で周辺冠動脈内径の4倍を越えるもの．

(b) 重症度分類

心エコー検査，ならびに選択的冠動脈造影検査等で得られた所見に基づいて，以下の5群に分類する．

Ⅰ．拡大性変化がなかった群：急性期を含め，冠動脈の拡大性変化を認めない症例．
Ⅱ．急性期の一過性拡大群：第30病日までに正常化する軽度の一過性拡大を認めた症例
Ⅲ．Regression群：第30病日においても拡大以上の瘤形成を残した症例で，発症後1年までに両側冠動脈所見が完全に正常化し，かつⅤ群に該当しない症例
Ⅳ．冠動脈瘤の残存群：冠動脈造影検査で1年以上，片側もしくは両側の冠動脈瘤を認めるが，かつⅤ群に該当しない症例
Ⅴ．冠動脈狭窄性病変群：冠動脈造影検査で冠動脈に狭窄性病変を認める症例．
(a) 虚血所見のない群：諸検査において虚血所見を認めない症例
(b) 虚血所見を有する群：諸検査において明らかな虚血所見を有する症例

参考条項：中等度以上の弁膜障害，心不全，重症不整脈などを有する症例については，各重症度分類に付記する．

表3　証拠のレベル

Level A（高）	多数の患者を対象とする多くの無作為臨床試験によりデータが得られている．
Level B（中）	少数の患者を対象とする限られた数の無作為試験，あるいは非無作為試験または観察的登録の綿密な分析からデータが得られている場合
Level C（低）	専門家の合意が勧告の主要な根拠となっている場合

表4　勧告の程度

Class I	検査・治療が有用・有効であることについて証明されているか，あるいは見解が広く一致している．
Class II	検査・治療の有用性・有効性に関するデータまたは見解が一致していない場合がある．
Class III	検査・治療が有用・有効ではなく，ときに有害となる可能性が証明されているか，あるいは有害との見解が広く一致している．